Infrared Spectra of the CH_3−CrF, CH_2=WHF, and CH≡WH_2F Molecules: Reversible Photochemical Interconversion by α-Hydrogen Transfer

Han-Gook Cho

Department of Chemistry, University of Incheon, 177 Dohwa-dong, Nam-ku, Incheon 402-749, South Korea

Lester Andrews*

Department of Chemistry, University of Virginia, P.O. Box 400319, Charlottesville, Virginia 22904-4319

Received July 21, 2005

Group 6 methylmetal fluoride, methylidene, and methylidyne complexes (CH_3−MF, CH_2=MHF, and CH≡MH_2F) are formed by reaction of the laser-ablated metal atoms and methyl fluoride during condensation in excess argon and have been identified by matrix infrared spectroscopy. The CH_3−CrF molecule is much more stable and is the only product found for Cr, and all three comparable energy products are observed for Mo, but only the more stable CH_2=WHF and CH≡WH_2F forms are trapped for W. The last molecules are photoreversible, owing to α-hydrogen transfer between carbon and metal atoms. The methylidene complexes are formed on ultraviolet irradiation (240−380 nm) at the expense of the methylidyne complexes, and the process is reversed on visible irradiation (λ > 420 nm). Calculations show that one α-H is distorted toward the metal atom, which provides evidence of strong agostic interaction in the methylidene ground state molecules.

Introduction

Laser-ablated group 4 metal atoms react with CH_3F to first form CH_3−MF, which rearrange to the simple methylidene hydride fluoride complexes (CH_2=MHF). These complexes reveal asymmetry in the CH_2 group and agostic bonding that is more pronounced with Ti than with Hf.[1−3] Substituted high-oxidation-state alkylidenes (R_1R_2C=M) and alkylidynes (RC≡M) have been investigated extensively in the last three decades, and many of these complexes are agostic.[4] These ligand-stabilized compounds are synthesized by intramolecular α-hydrogen transfer from a bis(alkyl) precursor, and they have found applications as catalysts for metathesis reactions of alkenes and alkynes.[5,6] The agostic interaction in methylidenes involves α-H to metal interaction and stabilization of the C=M double bond,[7−9] and simple methylidene model systems made from methyl halides will help understand this bonding interaction. Early computations have explored the effect of halogen substituents on simple methylidene complexes.[10]

Although stable alkylidene complexes of group 4 metals are limited, a large number of group 6 metal alkylidene complexes are known, and the higher group 6 valence supports the formation of related substituted alkylidyne complexes, which have no group 4 counterparts.[4] To investigate alkylidyne complexes, CH_3F has been reacted with group 6 atoms to produce simple methylmetal fluoride, methylidene, and methylidyne complexes. The Mo and CH_3F methylidene and methylidyne reaction products have recently been characterized,[11] and the Cr and W analogues are identified here through comparison of their matrix infrared spectra, their reversible photochemical interconversion, and DFT structure and frequency calculations.

Experimental and Computational Methods

The laser-ablation matrix-infrared experiment has been described previously.[12,13] In summary, laser-ablated group 6 metal atoms (Goodfellow, Johnson Matthey) were codeposited with CH_3F (Matheson), CD_3F (synthesized from CD_3Br and HgF_2),[14] and $^{13}CH_3F$ (Cambridge Isotopic Laboratories) in excess argon (MG Industries) on a CsI window at 8 K. Infrared

* To whom correspondence should be addressed. E-mail: lsa@virginia.edu.

(1) Cho, H.-G.; Andrews, L. *J. Phys. Chem. A* **2004**, *108*, 6294.
(2) Cho, H.-G.; Andrews, L. *J. Am. Chem. Soc.* **2004**, *126*, 10485.
(3) Cho, H.-G.; Andrews, L. *Organometallics* **2004**, *23*, 4357.
(4) Schrock, R. R. *Chem. Rev*. **2002**, *102*, 145.
(5) Choi, S.-H.; Lin, Z. *Organometallics* **1999**, *18*, 5488.
(6) Buchmeiser, M. R. *Chem. Rev*. **2000**, *100*, 1565.
(7) Ujaque, G.; Cooper, A. C.; Maseras, F.; Eisenstein, O.; Caulton, K. G. *J. Am. Chem. Soc*. **1998**, *120*, 361.
(8) (a) Eisenstein, O.; Jean, Y. *J. Am. Chem. Soc.* **1985**, *107*, 1177. (b) Clot, E.; Eisenstein, O. Agostic Interactions from a Computational Perspective. In *Structure and Bonding, Computational Inorganic Chemistry*, Kaltzoyannis, N., McGrady, J. E., Eds.; Springer-Verlag: Heidelberg, Germany, 2004; pp 1−36.
(9) Scherer, W.; McGrady, G. S. *Angew. Chem., Int. Ed.* **2004**, *43*, 1782.
(10) Cundari, T. R.; Gordon, M. S. *J. Am. Chem. Soc*. **1992**, *114*, 539.
(11) Cho, H.-G.; Andrews, L. *Chem. Eur. J.* **2005**, *11*, 5017 (Mo + CH_3F).
(12) Andrews, L.; Citra, A. *Chem. Rev.* **2002**, *102,* 885 and references therein.
(13) Wang, X.; Andrews, L. *J. Phys. Chem. A* **2003**, *107*, 570.
(14) Andrews, L.; Dyke, J. M.; Jonathan, N.; Keddar, N.; Morris, A.; Ridha, A. *J. Phys. Chem*. **1984**, *88*, 2364.

10.1021/om050613q CCC: $30.25
Publication on Web 10/12/2005

spectra were recorded at 0.5 cm^{-1} resolution on a Nicolet 550 spectrometer with a HgCdTe type B detector. Samples were irradiated by a mercury arc street lamp (175 W, globe removed) for 20 min periods and were annealed, and more spectra were recorded.

Density functional theory (DFT) calculations were done using the Gaussian 98 program, the B3LYP density functional, large 6-311++G(3df,3pd) basis sets for C, H, and F, and SDD effective core potential and basis set for metal atoms (14 valence electrons) for structures and vibrational frequencies of the expected reaction products.[15] The optimized geometry was confirmed by vibrational analysis. Complementary calculations were performed at the coupled-cluster (CCSD) level of electronic structure theory using the medium 6-311++G-(2d,p) basis set for the CH_2=MoHF and CH_2=WHF complexes to compare with DFT results.

Results

Infrared spectra and density functional calculations for Cr, Mo, and W atom reaction products with CH_3F will be presented.

Chromium. Laser-ablated Cr atoms react with CH_3F on codeposition in excess argon to form a single new product with infrared absorptions at 635.6, 553.8, and 500.6 cm^{-1}, which are marked I in Figure 1 and listed in Table 1. These bands increase 30% on visible (λ > 420 nm) irradiation and another 40% on near-ultraviolet and visible (λ > 290 nm) irradiation. The above bands decrease 10% upon exposure to 240−380 nm radiation, while a very weak 648.6 cm^{-1} absorption increases. The latter could be due to CrF, which has a 655.7 cm^{-1} fundamental in the gas phase.[16] Isotopic substitution displaces these product absorptions. Reaction with $^{13}CH_3F$ gives new bands at 635.2, 550.9, and 489.8 cm^{-1}, and reaction with CD_3F produces new bands at 633.3 and 476.5 cm^{-1}. In addition, these experiments formed intermediate species from CH_3F photodissociation that have been identified previously.[1,2,3,17]

Molybdenum. Molybdenum atoms excited by laser ablation react with CH_3F to produce three new species that are labeled I−III in Figure 2, as described previously.[11] The I and II bands decrease substantially on visible irradiation (λ > 420 nm), but near-ultraviolet irradiation (240−380 nm) restores I and doubles the yield of II. The II absorptions and isotopic modifications are listed in Table 2. The III absorptions, on the other hand, exhibit opposite photolysis behavior, which is to increase on visible and decrease on ultraviolet irradiation. The effect of three visible/ultraviolet irradiation cycles, shown in Figure 2, is completely reversible.

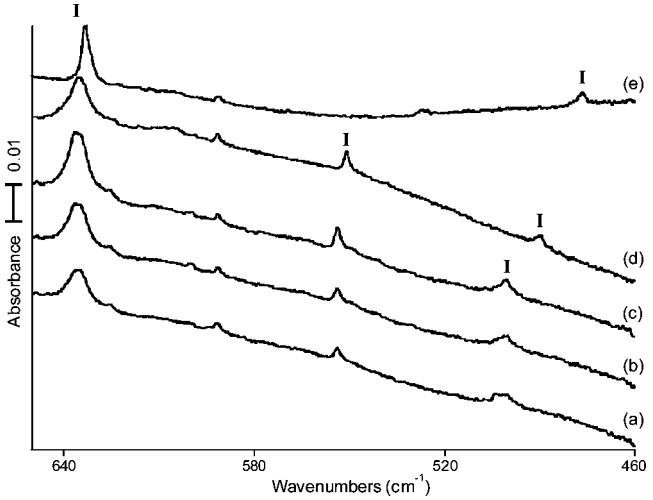

Figure 1. Infrared spectra in the 650−460 cm^{-1} region for the reaction product of laser-ablated Cr atoms and CH_3F molecules in excess argon: (a) Cr and 0.5% CH_3F codeposited for 60 min; (b) mixture as in (a) after λ > 420 nm irradiation for 20 min; (c) mixture as in (a) after λ > 290 nm irradiation; (d) Cr and 0.5% $^{13}CH_3F$ codeposited for 60 min and irradiated with λ > 320 nm; (e) Cr and 0.5% CD_3F codeposited for 60 min and irradiated with λ > 320 nm.

Tungsten. Laser-ablated W atoms combine with CH_3F to form two new products with infrared absorptions marked II and III in Figure 3, which are represented by two sharp III bands at 1936.4 and 1930.4 cm^{-1} and one II band at 1905.6 cm^{-1}. The other product absorptions in each group are included in Tables 3 and 4. These two products exhibit reversible photochemistry with visible and near-ultraviolet irradiation. Visible (λ > 420 nm) irradiation decreases the II bands by 20% and increases the III bands by 15%, whereas near-ultraviolet (240−380 nm) irradiation reverses these changes (Figure 3d−g).

A similar spectrum and photochemistry were observed with $^{13}CH_3F$, and the band positions are listed in Tables 3 and 4. The CD_3F precursor gave shifted absorptions and, notably, a single III band at 1386.4 cm^{-1} and a single II band at 1365.6 cm^{-1}, as shown in Figure 4.

Calculations. B3LYP density functional calculations were done for the anticipated set of reaction products CH_3−MH, CH_2=MHF, and CH≡MH_2F using the large 6-311++G(3df,3pd) basis set for H, C, and F and the SDD pseudopotential for metal atoms. The structures obtained are illustrated in Figure 5. Note the substantial agostic distortions for the CH_2 group in CH_2=MoHF and CH_2=WHF but very little distortion for CH_2=CrHF. Approximate energies for each product were computed relative to the metal atom and CH_3F, and these are displayed in Figure 6. Note that the relative product stabilities change within the group 6 family metals. Structures calculated for CH_2=MoHF and CH_2=WHF at the CCSD level of theory are similar to those calculated with DFT. The CCSD structural parameters follow for CH_2=MoHF (C−H, 1.081, 1.136 Å; C=Mo, 1.850 Å; Mo−H, 1.698 Å; Mo−F, 1.897 Å; agostic angle H−C−Mo, 82.4°; angle H−C−H, 116.0°; angle C−Mo−

(15) (a) Frisch, M. J.; Trucks, G. W.; Schlegel, H. B.; Scuseria, G. E.; Robb, M. A.; Cheeseman, J. R.; Zakrzewski, V. G.; Montgomery, J. A., Jr.; Stratmann, R. E.; Burant, J. C.; Dapprich, S.; Millam, J. M.; Daniels, A. D.; Kudin, K. N.; Strain, M. C.; Farkas, O.; Tomasi, J.; Barone, V.; Cossi, M.; Cammi, R.; Mennucci, B.; Pomelli, C.; Adamo, C.; Clifford, S.; Ochterski, J.; Petersson, G. A.; Ayala, P. Y.; Cui, Q.; Morokuma, K.; Malick, D. K.; Rabuck, A. D.; Raghavachari, K.; Foresman, J. B.; Cioslowski, J.; Ortiz, J. V.; Stefanov, B. B.; Liu, G.; Liashenko, A.; Piskorz, P.; Komaromi, I.; Gomperts, R.; Martin, R. L.; Fox, D. J.; Keith, T.; Al-Laham, M. A.; Peng, C. Y.; Nanayakkara, A.; Gonzalez, C.; Challacombe, M.; Gill, P. M. W.; Johnson, B. G.; Chen, W.; Wong, M. W.; Andres, J. L.; Head-Gordon, M.; Replogle, E. S.; Pople, J. A. *Gaussian 98*, revision A.11.4; Gaussian, Inc.: Pittsburgh, PA, 1998. (b) Stevens, P. J.; Devlin, F. J.; Chablowski, C. F.; Frisch, M. J. *J. Phys. Chem.* **1994**, *98*, 11623. (c) Krishnan, R.; Binkley, J. S.; Seeger, R.; Pople, J. A. *J. Chem. Phys.* **1980**, *72*, 650. Frisch, M. J.; Pople, J. A.; Binkley, J. S. *J. Chem. Phys.* **1984**, *80*, 3265. (d) Andrae, D.; Haussermann, U.; Daly, M.; Stoll, H.; Preuss, H. *Theor. Chim. Acta* **1990**, *88*, 123.

(16) Koivisto, R.; Wallin, S.; Launila, O. *J. Mol. Spectrosc.* **1995**, *172*, 464.

(17) Jacox, M. E.; Milligan D. E. *J. Chem. Phys.* **1969**, *50*, 3252.

Table 1. Observed and Calculated Fundamental Frequencies of CH_3−CrF in the Ground Electronic State ($^5A'$)[a]

	CH_3−CrF			CD_3−CrF			$^{13}CH_3$−CrF		
descripn	obsd	calcd[b]	int	obsd	calcd[b]	int	obsd	calcd[b]	int
A′ CH_3 str		3109.7	5		2302.1	1		3098.4	5
A′ CH_3 str		3072.0	12		2264.0	5		3062.9	13
A′ CH_3 str		2979.5	11		2138.9	3		2975.3	11
A′ CH_3 scis		1443.6	1		1048.3	1		1440.3	1
A′ CH_3 scis		1417.9	1		1029.4	2		1414.7	1
A′ CH_3 def		1154.3	5		899.0	2		1145.8	6
A′ Cr−F str	635.6	662.6	159	633.3	661.2	153	635.2	662.4	158
A′ Cr−CH_3 str	553.8	572.4	28	476.5	491.4	26	500.6	567.2	34
A″ CH_3 rock	500.6	570.0	34		426.1	23	489.8	564.7	26
A″ CrCH bend		456.7	17		377.2	12		448.5	17
A″ CH_3 rock		128.2	9		118.0	9		127.2	9
A″ CCrF bend		99.0	1		71.2	3		98.9	1

[a] Frequencies and intensities (int) are in cm^{-1} and km/mol, respectively. [b] B3LYP/6-311+G(3df,3pd)/SDD level.

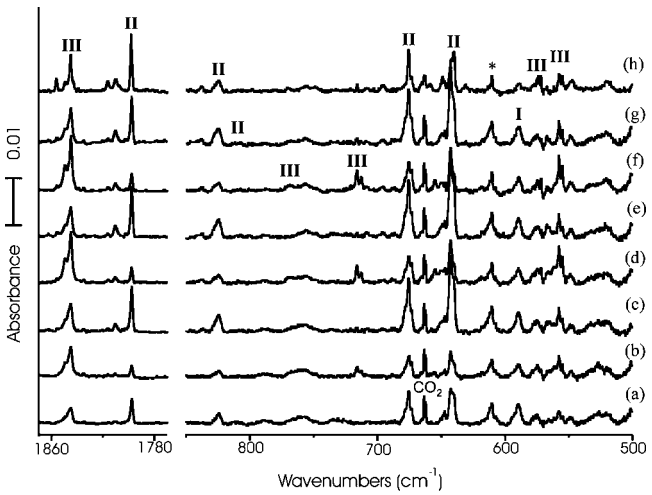

Figure 2. Infrared spectra for laser-ablated Mo atoms codeposited with CH_3F molecules in excess argon: (a) Mo + 0.5% CH_3F codeposited for 1 h; (b) mixture as in (a) after irradiation using a filter $\lambda > 420$ nm for 20 min; (c) mixture as in (a) after irradiation using a filter 240 nm $< \lambda <$ 380 nm; (d) mixture as in (a) after $\lambda > 420$ nm irradiation; (e) mixture as in (a) after 240−380 nm irradiation; (f) mixture as in (a) after $\lambda > 420$ nm irradiation; (g) mixture as in (a) after 240−380 nm irradiation,; (h) mixture as in (a) after annealing to 26 K. The absorption marked with an asterisk is not identified.

H, 107.2°; angle H−Mo−F, 120.1°) and for CH_2═WHF (C−H, 1.079, 1.135 Å; C═W, 1.867 Å; W−H, 1.707 Å; W−F, 1.897 Å; agostic angle H−C−W, 83.4°; angle H−C−H, 115.5°; angle C−W−H, 106.5°; angle H−W−F, 120.3°).

Frequencies were computed at the B3LYP level for these molecules to assist in assigning the experimental spectra. The three frequencies for CH_3−CrF with the largest infrared intensities were the Cr−F stretching mode at 662.6 cm^{-1} (159 km/mol infrared intensity), the symmetric CH_3 deformation, the C−Cr stretching mode at 572.4 cm^{-1} (28 km/mol), and the antisymmetric CH_3 deformation (or CH_3 rock) at 570.0 cm^{-1} (34 km/mol). These calculated frequencies shifted as shown in Table 1 for $^{13}CH_3$−CrF and CD_3−CrF. Computations with the medium basis set gave frequencies within +7 cm^{-1} of the large basis set values with two a few cm^{-1} closer and one a few cm^{-1} further from the observed values.

The most intense modes computed for CH_3−MoF are the Mo−F stretching mode at 628.8 cm^{-1} (148 km/mol) and the mostly C−Mo stretching mode at 448.6 cm^{-1} (23 km/mol).[11] The harmonic frequencies calculated for CH_2═MoHF are displayed in Table 2 for the planar triplet ground state molecule, and five of these modes have observable infrared intensity. Frequencies computed at the CCSD level of theory are compared in Table 2. The general agreement between B3LYP and CCSD frequencies supports their prediction for experimental frequencies. The isotopic shifts provide a measure of mode mixing, and the important mostly C═Mo stretching mode computed at 843.4 and 849.4 cm^{-1}, respectively, shows slightly more carbon-13 shift with B3LYP than with CCSD. Frequencies computed at the B3LYP level for CH≡MoH_2F in the singlet ground state with a symmetry plane have been reported, and six of these frequencies are observed in the matrix infrared spectra.[11]

Likewise, the most intense infrared mode for CH_3−WF is the W−F stretching mode calculated at 631.4 cm^{-1} (93 km/mol). The frequencies computed for CH_2═WHF in the triplet planar ground state are listed in Table 3 along with the approximate mode description. Three of these modes have considerable infrared intensity. Fundamental frequencies calculated for CH≡WH_2F in the singlet ground state are given in Table 4. Six of these modes have substantial infrared intensity.

Finally, similar calibration calculations were done for the simple MF diatomic molecules, and in all cases sextet states were lower than quartet states. We found a 641 cm^{-1} fundamental and 1.797 Å bond length for CrF, which are in very good agreement with 655.7 cm^{-1} and 1.784 Å experimental values.[16] We calculated a 607 cm^{-1} fundamental and 1.924 Å bond length for MoF and 623 cm^{-1} frequency and 1.920 Å bond length for WF. Unfortunately, no experimental values are available for MoF and WF.

Discussion

The group 6 metal−methyl fluoride reaction products will be identified from matrix infrared spectra with the assistance of isotopic substitution, photochemical behavior, and comparison to frequencies predicted by density functional theory calculations.

CH_3−MF. The group I absorptions are assigned to CH_3−CrF and CH_3−MoF. It is noteworthy that CH_3−CrF is by far the most stable Cr reaction product (Figure 6) and is the only product observed experimentally.

Table 2. Observed and Calculated Fundamental Frequencies of CH_2=MoHF Isotopomers in the Ground $^3A''$ Electronic State[a]

	CH_2=MoHF					CD_2=MoDF					$^{13}CH_2$=MoHF				
approx mode descripn	obsd	calcd[b]	int[b]	calcd[c]	int[c]	obsd	calcd[b]	int[b]	calcd[c]	int[c]	obsd	calcd[b]	int[b]	calcd[c]	int[c]
A′ C−H str		3233.6	7	3267.7	5		2397.0	7	2421.7	5		3222.4	7	3256.4	5
A′ C−H str		2759.2	5	2750.5	5		2007.5	4	2001.2	4		2753.0	5	2743.7	5
A′ Mo−H str	1797.7	1890.1	160	1928.9	180	1292.1	1344.4	83	1372.0	93	1797.7	1890.1	160	1928.9	180
A′ CH_2 bend		1368.5	23	1422.8	31		1066.8	17	1097.3	15		1360.1	24	1414.7	31
A′ C=Mo str	824.0	843.4	78	849.5	98	737.2	739.7	51	742.4	63	813.9	827.5	86	840.9	93
A′ CMoH bend	801.0	810.0	13	816.6	5	620.0	598.2	13	607.3	24	787.2	801.1	4	800.1	10
A′ Mo−F str	642.5	644.0	113	646.9	109	654.3	662.4	125	667.3	122	642.0	643.3	112	645.6	108
A′ CH_2 rock		525.7	16	566.2	34		397.2	7	424.7	11		522.7	15	563.9	33
A′ CMoF bend		195.9	2	194.4	3		179.2	2	178.4	3		194.2	2	192.3	3
A″ CH_2 wag	675.4	700.5	69	675.9	71	531.2	546.7	46	526.6	48	670.6	694.8	68	670.5	69
A″ CH o-o-p bend		449.0	14	431.4	18		327.8	5	316.3	6		449.0	14	431.4	18
A″ MoH o-o-p bend		94.1	44	137.5	54		71.8	25	103.2	31		93.8	44	137.2	34

[a] Frequencies and intensities are in cm^{-1} and km/mol, respectively. Infrared intensities are calculated values. [b] B3LYP/6-311++G(3df,3pd)/SDD level. [c] CCSD/6-311++G(2d,p)/SDD level.

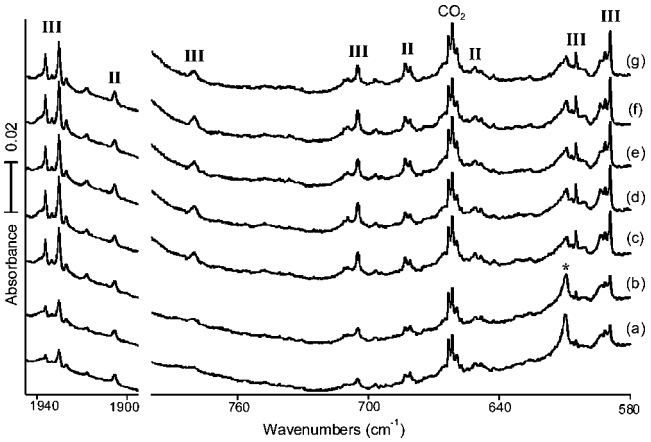

Figure 3. Infrared spectra in the 1945−1895 and 800−580 cm^{-1} regions for the reaction products of laser-ablated W atoms and CH_3F molecules in excess argon: (a) W and 5% CH_3F codeposited for 60 min, (b) mixture as in (a) after $\lambda > 420$ nm irradiation for 20 min; (c) mixture as in (a) after $\lambda > 290$ nm irradiation; (d) mixture as in (a) after $\lambda > 420$ nm irradiation; (e) mixture as in (a) after 240−380 nm irradiation; (f) mixture as in (a) after $\lambda > 420$ nm irradiation; (g) mixture as in (a) after 240−380 nm irradiation.

Although CH_3−MoF is barely the most stable Mo reaction product, CH_2=MoHF and CH≡MoH_2F are close in energy and all three are observed. However, CH_3−WF is the highest energy of the possible W reaction products, and CH_3−WF is not trapped in these matrix isolation experiments.

The three new absorptions observed with Cr and CH_3F at 635.6, 553.8, and 500.6 cm^{-1} (Figure 1) can be assigned to the three strongest absorptions computed for CH_3−CrF (Table 1). The most intense of these calculated at 662.6 cm^{-1} and observed at 635.6 cm^{-1} is due to the Cr−F stretching mode, which shows small shifts with $^{13}CH_3F$ and CD_3F in accord with the calculated values. We note that CrF itself exhibits a gaseous 655.7 cm^{-1} fundamental frequency.[16] The weaker 553.8 cm^{-1} band shifts 2.9 cm^{-1} with ^{13}C and 77.3 cm^{-1} with D substitution, and the computed mixed CH_3 deformation, C−Cr stretching mode at 572.4 cm^{-1} shifts 5.2 cm^{-1} with ^{13}C and 81.0 cm^{-1} with D in the harmonic approximation. The weak 500.6 cm^{-1} band shifts 10.8 cm^{-1} with ^{13}C, and the CH_3 rock computed at 570.0 cm^{-1} shifts 5.3 cm^{-1}. There is apparently slightly more mode mixing for the latter mode than is recognized by the calculation. Overall the agreement between observed band positions and isotopic frequency shifts and computed values is very good, and this substantiates our identification of the CH_3−CrF product.

In the Mo system two group I absorptions at 589.3 and 441.4 cm^{-1} have been assigned to CH_3−MoF.[11] The two strongest infrared absorbing modes are predicted at 628.8 cm^{-1} (148 km/mol) (mostly Mo−F stretching mode) and 448.6 cm^{-1} (23 km/mol) (mostly C−Mo stretching mode) for CH_3−MoF.

We have no spectroscopic evidence for CH_3−WF, as this molecule apparently rearranges spontaneously to the more stable methylidene complex.

CH_2=MHF. The group II infrared bands are assigned to CH_2=MoHF and to CH_2=WHF. Recall that group II absorptions for both metals decreased on visible irradiation in favor of group III and markedly increased on near-ultraviolet irradiation at the expense of group III.

The observed and calculated CH_2=MoHF frequencies are compared in Table 1, and the agreement is very good for five frequencies.[11] The strong band at 1797.7 cm^{-1} shifts to 1292.1 cm^{-1} on deuterium substitution, and this H/D ratio (1.391) is typical of heavy metal hydrides, as is the scale factor (observed/calculated = 1797.7/1890.1 = 0.951).[18,19] Four associated weaker absorptions are fit well by calculated frequency positions and isotopic shifts. The 824.0 cm^{-1} band decreases to 813.9 cm^{-1} with $^{13}CH_3F$ and to 737.2 cm^{-1} with CD_3F, and these 10.1 and 86.8 cm^{-1} shifts are comparable to the 15.9 and 103.7 cm^{-1} shifts predicted by B3LYP and 8.6 and 107.1 cm^{-1} shifts predicted by CCSD, where anharmonicity plays a role in the H/D comparison. Note that the B3LYP calculation predicts more of a carbon-13 shift than is observed and the CCSD calculation less. A pure diatomic C=Mo oscillator at this frequency would exhibit a 28.7 cm^{-1} carbon-13 shift; therefore, this C=Mo stretching mode is heavily mixed with the adjacent C−Mo−H bending mode, as shown by the large deuterium shift. The next weak 801.0 cm^{-1} absorption is displaced 13.8 cm^{-1} with $^{13}CH_3F$ and 181.0 cm^{-1} with CD_3F, and the predicted C−Mo−H bend at 810.0 cm^{-1} compares favorably with the B3LYP computed 9.0 and 221.8 cm^{-1} and CCSD computed 16.5 and 209.3 cm^{-1} shifts using the harmonic approximation. The strong

(18) Bytheway, I.; Wong, M. W. *Chem. Phys. Lett.* **1998**, *282*, 219.
(19) Scott, A. P.; Radom, L. *J. Phys. Chem.* **1996**, *100*, 16502.

Table 3. Observed and Calculated Fundamental Frequencies of CH_2=WHF Isotopomers in the Ground Electronic State ($^3A''$)[a]

	CH_2=WHF					CD_2=WDF					$^{13}CH_2$=WHF				
approx mode descripn	obsd	calcd[b]	int[b]	calcd[c]	int[c]	obsd	calcd[b]	int[b]	calcd[c]	int[c]	obsd	calcd[b]	int[b]	calcd[c]	int[c]
A′ C−H str		3248.9	7	3283.8	6		2409.0	8	2434.8	6		3237.5	7	3273.2	5
A′ C−H str		2750.7	6	2760.5	7		2002.3	5	2009.8	5		2744.4	6	2754.2	6
A′ W−H str	1905.6	1969.2	112	2020.2	132	1365.6	1397.2	57	1433.3	67	1905.6	1969.2	112	2020.1	132
A′ CH_2 bend		1368.6	22	1419.6	25		1069.8	15	1100.2	13		1359.9	22	1411.1	26
A′ C=W str		860.6	41	860.1	52	751.6	751.3	26	756.6	32		838.1	43	838.8	60
A′ CWH bend		790.6	28	806.5	34		581.1	5	591.4	6		786.8	25	801.0	24
A′ W−F str	651.2	644.4	100	652.5	95	656.8	656.4	133	665.1	148	648.2	643.9	100	651.6	95
A′ CH_2 rock		533.8	20	569.9	36		405.7	6	430.9	8		530.4	19	566.9	34
A′ CWF bend		182.4	1	188.0	2		165.3	1	172.1	2		180.3	1	185.8	2
A″ CH_2 wag	683.4	714.6	58	677.6	57	525.3	556.9	38	527.5	38	678.4	708.9	57	672.2	56
A″ CH o-o-p bend		420.8	14	399.9	20		307.2	6	293.1	8		420.8	14	399.9	20
A″ WH o-o-p bend		95.1	27	111.1	32		71.1	15	82.5	18		94.9	27	110.9	32

[a] Frequencies and intensities are in cm^{-1} and km/mol, respectively. Infrared intensities are calculated values. [b] B3LYP/6-311++G(3df,3pd)/SDD level. [c] CCSD/6-311++G(2d,p)/SDD level.

Table 4. Observed and Calculated Fundamental Frequencies of CH≡WH_2F Isotopomers in the Ground Electronic State ($^1A'$)[a]

	CH≡WH_2F			CD≡WD_2F			^{13}CH≡WH_2F	
approx mode descripn	obsd	calcd	int.	obsd	calcd	int.	obsd	calcd
A′ C−H str		3235.0	15		2405.9	13		3224.0
A′ WH_2 str	1930.4	2001.2	117	1386.4	1418.1	60	1930.3	2001.2
A′ C≡W str		1050.7	12		1002.0	10		1016.0
A′ WH_2 bend	780.4	806.2	67	682.3	676.7	112	780.2	806.0
A′ WH_2 wag	705.1	726.8	52	532.6	571.9	13	701.7	722.3
A′ W−F str		669.0	22		541.5	22		668.0
A′ WCH bend	589.3	606.4	103		452.5	34	588.4	605.8
A′ CWF bend		253.4	4		237.7	4		249.5
A″ WH_2 str	1936.4	1994.4	178	1386.4	1417.7	92	1936.3	1994.4
A″ CH o-o-p bend		801.7	8		635.8	7		794.0
A″ WH_2 deform	605.0	627.8	71		446.1	36	605.0	627.8
A″ WH_2 rock		419.1	0		313.1	0		418.9

[a] B3LYP/6-311++G3df,3pd/SDD level. Frequencies and intensities are in cm^{-1} and km/mol, respectively. Infrared intensities are calculated values.

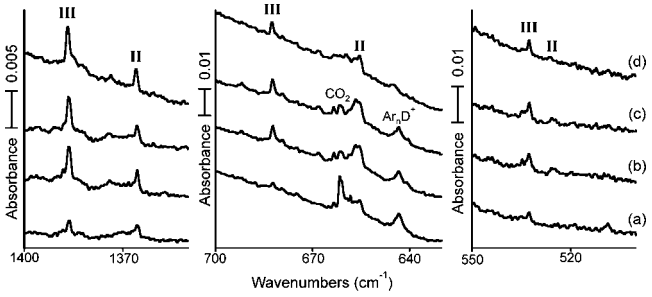

Figure 4. IR spectra in the 1400−1350, 700−630, and 550−500 cm^{-1} regions for laser-ablated W atoms codeposited with CD_3F in excess argon: (a) W and 0.5% CD_3F codeposited for 60 min; (b) mixture as in (a) after 240−380 nm irradiation for 20 min; (c) mixture as in (a) after λ > 420 nm irradiation; (d) mixture as in (a) after annealing to 26 K.

675.4 cm^{-1} peak red shifts 4.8 cm^{-1} with $^{13}CH_3F$ and 144.2 cm^{-1} with CD_3F, and the B3LYP computed 700.5 cm^{-1} CH_2 out-of-plane wag red-shifts 5.7 and 153.8 cm^{-1} and the CCSD computed 675.9 cm^{-1} wag shifts 5.4 and 149.3 cm^{-1} with major discrepancy due to the harmonic approximation. The strong 642.5 cm^{-1} band shifts −0.5 cm^{-1} with $^{13}CH_3F$ and +11.8 cm^{-1} with CD_3F, and the predominantly Mo−F stretching mode B3LYP computed at 644.0 cm^{-1} has −0.7 cm^{-1} red and +18.4 cm^{-1} isotopic displacements and CCSD computed shifts of −1.3 and +20.4 cm^{-1}. Mixing between close in-plane modes is responsible for the unusual blue deuterium shift. The 801.0 and 642.5 cm^{-1} normal modes for CH_2=MoHF are

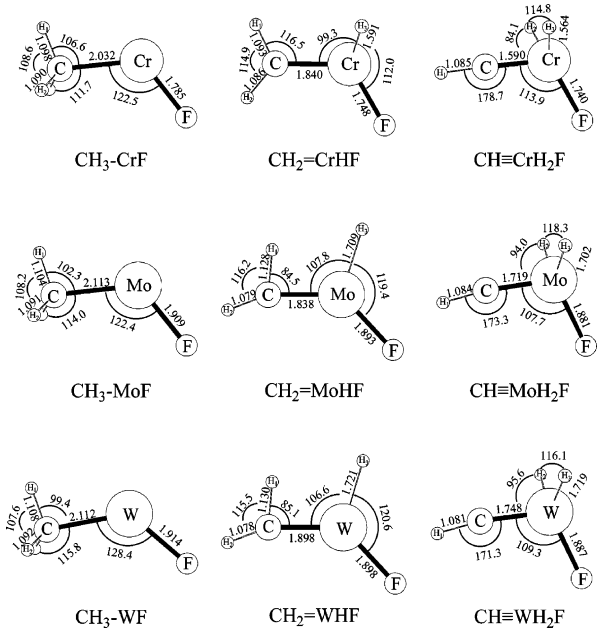

Figure 5. Structures computed for the group 6 CH_3−MF, CH_2=MHF, and CH≡MH_2F molecules at the B3LYP/6-311++G(3df,3pd)/SDD level of theory. Bond distances are given in angstroms and bond angles in degrees.

mostly C−Mo−H bend and Mo−F stretch coordinates, respectively, and deuterium substitution shifts the C−Mo−D bend *below* the Mo−F stretch. Therefore, the CD_2=MoDF normal modes are different internal coor-

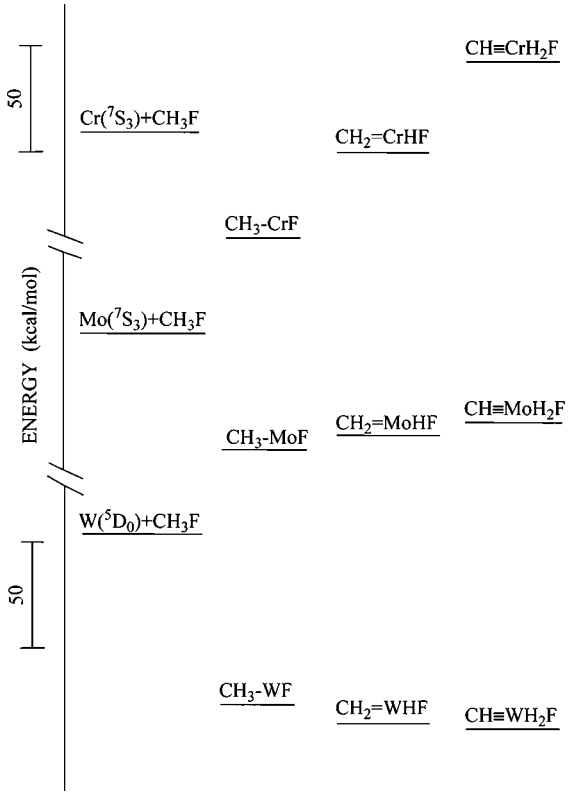

Figure 6. Relative energies of the lowest electronic states of the group 6 CH_3-MF, $CH_2=MHF$, and $CH\equiv MH_2F$ reaction product molecules that are involved in the reversible α-H transfer photochemistry.

dinate mixtures, which gives rise to a blue shift and more intensity for the 654.3 cm^{-1} absorption.

The observed and B3LYP and CCSD calculated $CH_2=$WHF frequencies are likewise compared in Table 3. The highest band at 1905.6 cm^{-1} shifts to 1365.6 cm^{-1} with CD_3F, and this H/D ratio (1.393) and the scale factor (1905.6/1969.2 = 0.968) are expected for heavy metal hydrides.[18,19] Two weaker absorptions at 651.2 and 683.2 cm^{-1} are well-described by our calculations. As for $CH_2=$MoHF, the mostly W−F stretching mode at 651.2 cm^{-1} is mixed with C−W−H bending and the C−W−D bend shifts below the W−F stretch and alters the normal mode, giving rise to blue shift and more intensity, as described by the calculations. The 5.6 cm^{-1} blue deuterium shift is predicted to be 12.0 cm^{-1} by B3LYP and 12.6 cm^{-1} by CCSD. The CH_2 wag at 683.4 cm^{-1} shifts 5.0 cm^{-1} with $^{13}CH_2$ and 157.9 cm^{-1} with CD_2, the B3LYP computed 714.6 cm^{-1} band shifts 5.7 and 157.7 cm^{-1}, and the CCSD computed 677.6 cm^{-1} band shifts 5.4 and 150.1 cm^{-1}. This excellent agreement between observed and calculated frequencies and isotopic shifts confirms our assignments to $CH_2=$WHF.

The $CH_2=$WHF complex identified here has a 1.898 Å computed C=W double-bond length. This is near the 1.88−1.975 Å range for C=W bonds in heavily ligated and substituted W methylidene complexes reviewed by Schrock.[4]

The $CH_2=$MoHF and $CH_2=$WHF structures illustrated in Figure 5 show distortion of the CH_2 subgroup and agostic bonding interaction to stabilize the C=Mo and C=W double bonds. The agostic H−C−M angle for the Mo methylidene, 84.5°, is considerably smaller than the 96.3° value computed for $CH_2=$ZrHF, and the agostic angle for the W methylidene, 85.1°, is likewise smaller than the 101.0° value computed for $CH_2=$HfHF.[3] Hence, we conclude that $CH_2=$MoHF and $CH_2=$WHF exhibit a stronger agostic interaction than $CH_2=$ZrHF and $CH_2=$HfHF. The Mulliken charges computed on Mo and W in these methylidenes, 1.68 and 1.66, respectively (Table 5), are higher than values for the Zr and Hf species, 1.36 and 1.18, respectively, and the C=M bonds are 0.13−0.09 Å shorter for the group 6 methylidenes.[3] The former complexes are planar at the metal center, but the latter are nonplanar. These methylidene complexes distort in order to stabilize the C=M double bond.[7−9]

The CCSD calculations give essentially the same structures for $CH_2=$MoHF (0.012 Å longer C=Mo bond and 2.1° smaller agostic angle) and $CH_2=$WHF (0.031 Å shorter C=W bond and 1.7° smaller agostic angle) as B3LYP (Figure 5). Although this comparison is reassuring, the T1 diagnostics 0.0526 and 0.0413 suggest that a proper electronic description may require a multireference calcuation.[20] Our main concern here is frequency prediction for experimental verification, and both calculations predict frequencies in reasonable agreement[18,19] with the observed values. A recent CCSD calculation found an agostic structure for $CH_2=WH_2$ with comparable C=W (1.874 Å) and agostic H−C−W angle (91.0°) values.[21]

$CH\equiv MH_2F$. The group III bands, which increase on visible photolysis, can be assigned definitively to the methylidyne complexes $CH\equiv MoH_2F$ and $CH\equiv WH_2F$ from six fundamental frequencies for each molecule. The case for $CH\equiv MoH_2F$ has been discussed[11] and is only summarized here in the upper region for comparison. The leading 1844.8 cm^{-1} band gives two counterparts at 1322.1 and 1330.5 cm^{-1} on deuteriation. Calculations find two Mo−H stretching modes within 2 cm^{-1} and two Mo−D stretching modes separated by 9.6 cm^{-1}, with the higher frequency antisymmetric stretching mode being 50% stronger.[11] Thus, the 1322.1 and 1330.5 cm^{-1} deuterium counterpart product bands separated by 8.4 cm^{-1} are in agreement. The 1844.8 cm^{-1} absorption is due to both antisymmetric and symmetric Mo−H_2 stretching modes of $CH\equiv MoH_2F$, and the scale factor (1844.8/1940.1 = 0.951) is in agreement with that found for $CH_2=$MoHF. The stronger 1330.5 cm^{-1} band arises from the antisymmetric Mo−D_2 stretching mode and the 1322.1 cm^{-1} band from the symmetric Mo−D_2 stretching motion of $CD\equiv MoD_2F$.

The evidence for $CH\equiv WH_2F$ is collected in Table 4. Two leading bands at 1936.4 and 1930.4 cm^{-1} give way on deuteriation to a single 1386.4 cm^{-1} absorption (Figures 3 and 4). Our calculations predict the stronger antisymmetric W−H_2 stretch in $CH\equiv WH_2F$ to be 6.8 cm^{-1} higher than the weaker symmetric stretch, and we observe a 6.0 cm^{-1} band separation. In the $CD\equiv WD_2F$ case, our computation predicts these modes only 0.4 cm^{-1} apart, and we observe a single band. As for $CH\equiv MoH_2F$, the weak C≡W stretching mode is covered by a CH_3F precursor absorption. The H−W−H valence angle bending mode is observed at 780.4 cm^{-1} with 0.2 cm^{-1} ^{13}C and 98.1 cm^{-1} D shifts, and the computed mode

(20) Lee, T. J.; Taylor, P. C. *Int. J. Quantum Chem. Symp.* **1989**, *23*, 199.

(21) Cho, H.-G.; Andrews, L.; Marsden, C. *Inorg. Chem.* **2005**, *44*, 7634.

Table 5. Mulliken Charges Calculated for the Group 6 CH_3-MF, $CH_2=MHF$, and $CH\equiv MH_2F$ Molecules[a]

	CH_3-CrH	$CH_2=CrHF$	$CH\equiv CrH_2F$	CH_3-MoF	$CH_2=MoHF$	$CH\equiv MoH_2F$	CH_3-WF	$CH_2=WHF$	$CH\equiv WH_2F$
M	1.108	1.274	1.217	1.239	1.679	1.800	1.263	1.662	1.962
F	−0.568	−0.530	−0.545	−0.607	−0.658	−0.609	−0.626	−0.657	−0.652
C	−0.605	−0.593	−0.458	−0.844	−0.740	−0.697	−0.830	−0.704	−0.742
H_1	0.033	0.042	0.144	0.079	0.011	0.070	0.084	−0.012	0.060
H_2	0.016	0.050	−0.179	0.066	0.033	−0.282	0.055	0.032	−0.314
H_3	0.016	−0.242	−0.179	0.066	−0.326	−0.282	0.055	−0.321	−0.314

[a] B3LYP/6-311++G(3df,3pd)/SDD level.

at 806.2 cm^{-1} shifts 0.2 and 129.5 cm^{-1}. The WH_2 wag at 705.1 cm^{-1} shifts 3.4 cm^{-1} with ^{13}C and 172.5 cm^{-1} with all-D, and the computed mode at 726.8 cm^{-1} shifts 4.5 and 159.9 cm^{-1}, respectively. The discrepancies between calculated and observed deuterium shifts for these two nearby modes of the same symmetry are probably due to mode mixing slightly different from that modeled by the calculation, which is, of course, in the harmonic approximation. The W−C−H bending mode observed at 589.3 cm^{-1} with 0.9 cm^{-1} ^{13}C shift is predicted at 606.4 cm^{-1} with 0.6 cm^{-1} ^{13}C displacement. The strong $W-H_2$ deformation at 605.0 cm^{-1} is calculated at 627.8 cm^{-1}, both with no ^{13}C shift. Again, the excellent agreement found between six calculated and observed frequencies substantiates the identification and preparation of $CH\equiv WH_2F$.

The $CH\equiv WH_2F$ methylidyne characterized here has a B3LYP calculated 1.748 Å C≡W triple-bond length. This is in the range of C≡W triple-bond lengths calculated for the simple $CH\equiv WH_3$ molecule (1.742 Å)[21] and measured for tungsten−methylidyne complexes (1.746, 1.757 Å).[4]

Group 6 Comparisons. Interesting comparisons between the Cr, Mo, and W compounds can be made in Figure 6 and Tables 3−5. The stable Mo and W methylidynes have almost the same structures, where the bonds to W are very slightly longer. The W−H stretching frequencies are about 90 cm^{-1} higher than the Mo−H counterparts, and this is in accord with the binary hydrides.[22] The WH_2 valence angle bending mode is about 10 cm^{-1} higher than the MoH_2 value, but the WH_2 wag falls 10 cm^{-1} below the MoH_2 value. The W−C−H bending mode comes about 20 cm^{-1} above the corresponding Mo−C−H frequency, and the WH_2 deformation is approximately 30 cm^{-1} higher than the $Mo-H_2$ counterpart. The above frequency comparisons for $CH\equiv MoH_2F$ and $CH\equiv WH_2F$ are based on both experiment and computation, which again underscores excellent agreement between the two methods. Finally, Mulliken charges for the group 6 product and potential product compounds are compared in Table 5. The high energies of $CH_2=CrHF$ and $CH\equiv CrH_2F$ and their absence from the product spectrum is suggested by the failure of Cr to support the positive charge that Mo and W do for the methylidenes and most particularly the methylidynes.

Laser-ablated group 6 metal atoms contain sufficient excess energy to overcome any activation barrier for insertion reaction with CH_3F to produce CH_3-MF molecules. In the case of Cr the relative energies of other possible products (Figure 6) are too high, and the Cr + CH_3F reaction terminates with CH_3-CrF (Scheme 1). Thus, visible irradiation increases the yield of CH_3-CrF. In contrast, the three Mo products have comparable energies and $CH_2=MoHF$ and $CH\equiv MoH_2F$ result from successive α-H transfers[23] in the energized $[CH_3-MoF]^*$ and $[CH_2MoHF]^*$ intermediates first formed. Thus, visible irradiation decreases the CH_3-MoF first product. In the case of W the relative energies of other products are lower, and the W + CH_3F reaction proceeds directly to $CH_2=WHF$ and $CH\equiv WH_2F$ (Scheme 1). Even though CH_3F has three C−H bonds to complete with one C−F bond for insertion, the CH_2F-MH product is much higher in energy, based on our previous computations for the triplet CH_2F-ZrH and CH_2F-MoH molecules.[3,11] The distribution among the group 6 metal products observed here is in keeping with that for ligated methylidene and methylidyne complexes: few Cr examples, many Mo, and very many W compounds are known.[4] Finally, a similar relationship has been observed for the analogous group 6 metal reaction products with methane in excess argon.[21] However, an early investigation of photoexcited Cr atoms in pure solid methane failed to produce an insertion product, although several later transition-metal atoms did form CH_3MH products.[24]

Scheme 1

$$Cr\ (^7S) + CH_3F \xrightarrow{UV} CH_3-CrF$$

$$Mo\ (^7S) + CH_3F \xrightarrow{UV}$$

$$CH_3-MoF \underset{UV}{\overset{vis}{\rightleftharpoons}} CH_2=MoHF \underset{UV}{\overset{vis}{\rightleftharpoons}} CH\equiv WH_2F$$

$$W\ (^5D) + CH_3F \xrightarrow{UV}$$

$$CH_3-WF \rightarrow CH_2=WHF \underset{UV}{\overset{vis}{\rightleftharpoons}} CH\equiv WH_2F$$

We employ photochemistry to interconvert and group the major product absorptions from the activation of CH_3F by Mo and W atoms. Visible irradiation of the initial sample containing all three Mo products halves I and II and doubles III. Thus, by two successive α-H transfers $CH_2=MoHF$ and $CH\equiv MoH_2F$ are formed from CH_3-MoF. Subsequent ultraviolet irradiation reverses the process, but $CH_2=MoHF$ is tripled and CH_3-MoF only doubled as $CH\equiv MoH_2F$ is decreased slightly, since one hydrogen on Mo is returned to carbon more easily than two. Similarly, $CH_2=WHF$ and $CH\equiv WH_2F$ are interconverted by visible and UV light (Scheme 1). The ultraviolet irradiation contains the resonance absorptions of Mo and W in solid argon,[25,26] and this excitation

(22) Andrews, L. *Chem. Soc. Rev.* **2004**, *33*, 123.

(23) Crabtree, R. H. *The Organometallic Chemistry of the Transition Metals*; Wiley: New York, 2001, p 190.

(24) Billups, W. E.; Konarski, M. M.; Hauge, R. H.; Margrave, J. L. *J. Am. Chem. Soc.* **1980**, *102*, 7394.

(25) Pellin, M. J.; Gruen, D. M.; Fisher, T.; Foosnaes, T. *J. Chem. Phys.* **1983**, *79*, 5871.

can promote the insertion reaction to form more CH_3−MoF and CH_3−WF, which can undergo further rearrangements. The infrared spectra indicate that these α-H transfer reactions are completely reversible.

Conclusions

Laser-ablated group 6 metal atoms react with methyl fluoride molecules during condensation in excess argon to form the methylmetal fluoride, methylidene, and methylidyne complexes (CH_3−MF, CH_2═MHF, and CH≡MH_2F). Computed relative product energies help to explain the product distribution for each metal. The substantially more stable CH_3−CrF molecule is the only product observed for Cr, all three products are of similar energy for Mo and all are observed in these experiments, and only the more stable CH_2═WHF and CH≡WH_2F forms are trapped in the argon matrix. These last molecules are photoreversible via α-hydrogen migration between carbon and metal atoms. The methyl and methylidene complexes are formed on ultraviolet irradiation (240−380 nm), while the methylidyne complex is destroyed, and the process is reversed on visible irradiation (λ > 420 nm). Electronic structure calculations show that one of the α-hydrogen atoms in the methylidene complexes is distorted (B3LYP, ∠HCMo = 84.5°, ∠HCW = 85.1°) toward the metal atom, which provides evidence of strong agostic interaction in the triplet ground states that is stronger in the group 6 than in the group 4 methylidene hydride fluoride complexes. The calculated C≡M bond length in the singlet ground-state methylidyne complexes is in the range of triple-bond measurements for known methylidyne complexes.[4] These simple molecules are identified from matrix infrared spectra through isotopic substitution and matching with vibrational frequencies computed by DFT and CCSD to be intense infrared absorptions.

The structures and frequencies computed for CH_2═MoHF and CH_2═WHF at the CCSD and B3LYP levels of theory are comparable, which justifies the use of the less time-consuming DFT method. The M−H stretching frequencies for these methylidene complexes are 3−5% higher using B3LYP and 6−7% higher with CCSD than observed values; both calculations are within 2−3 cm^{-1} for the Mo−F stretching mode, but CCSD provides a slightly more accurate prediction than B3LYP for the W−F stretching mode and the CH_2 wagging modes.

Acknowledgment. We appreciate support from NSF Grant CHE 03-52487 to L.A.

OM050613Q

(26) Schoch, R.; Kay, E. *J. Chem. Phys.* **1973**, *59*, 718.